

Study on the joining of ceramic matrix composites to an Al alloy for advanced brake systems

*Original*

Study on the joining of ceramic matrix composites to an Al alloy for advanced brake systems / Casalegno, Valentina; Smeacetto, Federico; Salvo, Milena; Sangermano, Marco; Bairo, Francesco; Noé, Camilla; Orlandi, Marco; Piavani, Riccardo; Bonfanti, Roberto; Ferraris, Monica. - In: CERAMICS INTERNATIONAL. - ISSN 0272-8842. - ELETTRONICO. - 47:(2021), pp. 23463-23473. [10.1016/j.ceramint.2021.05.062]

*Availability:*

This version is available at: 11583/2903192 since: 2021-05-28T14:18:31Z

*Publisher:*

elsevier

*Published*

DOI:10.1016/j.ceramint.2021.05.062

*Terms of use:*

This article is made available under terms and conditions as specified in the corresponding bibliographic description in the repository

*Publisher copyright*

Elsevier postprint/Author's Accepted Manuscript

© 2021. This manuscript version is made available under the CC-BY-NC-ND 4.0 license  
<http://creativecommons.org/licenses/by-nc-nd/4.0/>. The final authenticated version is available online at:  
<http://dx.doi.org/10.1016/j.ceramint.2021.05.062>

(Article begins on next page)

# Study on the joining of ceramic matrix composites to an Al alloy for advanced brake systems

*Valentina Casalegno<sup>1\*</sup>, Federico Smeacetto<sup>1</sup>, Milena Salvo<sup>1</sup>, Marco Sangermano<sup>1</sup>, Francesco Baino<sup>1</sup>, Camilla Noé<sup>1</sup>, Marco Orlandi<sup>2</sup>, Riccardo Piavani<sup>2</sup>, Roberto Bonfanti<sup>2</sup>, Monica Ferraris<sup>1</sup>*

<sup>1</sup> *Department of Applied Science and Technology (DISAT), Politecnico di Torino*

*Corso Duca degli Abruzzi 24-10129 Torino, Italy*

<sup>2</sup> *BSCCB- Brembo SGL Carbon Ceramic Brakes, viale Europa 2 24040 Stezzano (BG), Italy*

Corresponding author: [valentina.casalegno@polito.it](mailto:valentina.casalegno@polito.it)

Keywords: composites; joining; functional applications

## Abstract

This work addresses the integration of ceramic matrix composites (CMCs) and an Al alloy to obtain mechanically reliable and in-service durable CMC-Al alloy joints for high-performance road brake discs. Such a braking system is based on the use of CMC discs mounted onto a hub or stub axle by means of a mounting bell, manufactured in aluminium alloy. The CMCs, developed by Brembo SGL Carbon Ceramic Brakes (BSCCB), consist of an Si-SiC matrix reinforced with short carbon fibre bundles.

An epoxy adhesive, Supreme 42HT-2, whose curing parameters had been characterised to establish the best joining process, was chosen as a potential joining material as it showed the most promising results. CMC/ Supreme 42HT-2 /Al alloy joined samples, obtained following the supplier's recommended curing process, exhibited a shear strength of  $31.6 \pm 7.2$  MPa, while samples processed with a post thermal treatment at 200 °C for 10 minutes showed a value of  $38.2 \pm 6.4$  MPa. The influence of corrosion, in a high-salinity environment, on the mechanical strength of the joined samples is also reviewed and discussed. Thermal cycles (from room temperature to 200°C) and the corrosive environment did not affect the mechanical properties of the joints or the failure propagation mode to any great extent.

## 1. Introduction

Ceramic matrix composites (CMCs) are considered as key materials for brake systems because of their outstanding performances and significant weight savings over traditional cast iron discs [1, 2]. Moreover, they can provide exceptional braking power to several vehicles, e.g. high-performance cars, and offer higher strength and thermal conductivity, lower wear and higher fading stability than traditional options [3].

A considerable amount of literature has been published on CMCs for braking systems, and different manufacturing routes and methods [ 4-7 ] have been highlighted to improve oxidation resistance, which is the main factor that has to be considered when using these materials. C and SiC-based composites have in particular received considerable attention, because of their superior friction behaviour, especially in ventilated brake discs.

However, CMCs also suffer from some technological limitations, due to the difficulty of their assembly with metallic parts.

A brake disc assembly is usually made up of a brake disc ring connected to a brake disc bell. In the present study, the disc is made of CMC, while the disc bell is metallic (an Al alloy). Such a design is much lighter than a single component made up of a disc and a bell in one piece, without connecting elements, and it allows the risk of distortion, due to thermal expansion of the disc, to be reduced. This becomes important in the case of a large disc and it is considered essential for braking systems with a larger diameter than 330 mm.

A brake disc bell is usually connected to a brake disc ring by different connecting elements, i.e. the integration is obtained by means of mechanical joining (pins, threaded bolts, etc) [8, 9]. Non-permanent connections, obtained by means of the interlocking of metal with ceramic subcomponents, are commonly used. However, adhesives or brazing

alloys are preferable in the case of surfaces that are not flat and for complex geometries, and to optimise the component design.

The brazing of ceramic onto aluminium alloys cannot be considered a well-established technology. It in fact suffers from two main issues: 1) the metal filler does not usually form a strong spontaneous bond at the interface with the ceramic part, since the brazing temperatures are relatively low (below the melting point of the Al alloy) and specific active metal brazes are therefore required, 2) large thermal stresses are generated at the interface after the assembly cools to room temperature, due to the different shrinkages of the materials. Furthermore, the joining process in the selected brake system should be lower than 200° C to avoid ultra-ageing or annealing of the aluminium alloy, which can lead to detrimental effects on its mechanical properties [10].

For this reason, an interesting alternative is the use of adhesive joining, which is a very flexible technique, as it rules out the need for any additional elements for mechanical connections, such as bolts, rivets, etc., which would increase the weight of the joined structure. Joining processes that involve the use of adhesives are cold processes, compared to brazing technologies and, in recent years, adhesive bonding has been used more and more for the joining of a variety of components [11-13] and extensively in the automotive field [14], thereby reducing the detrimental effects of heat during the joining process. Moreover, adhesive joining is cheaper than other processes and leads to improved crash performances/safety [15].

It is worth pointing out that the stress concentrations that are present in riveted joints are avoided to a great extent in adhesive joints, because the stresses are distributed over a far larger area, and the adhesives make it possible to join brittle structures which could otherwise be damaged by riveting, such as ceramic-based materials.

Adhesives are commonly employed in the aerospace, automotive and building industries to join elements made of dissimilar materials [16]. The best known and most

widely used structural adhesives are epoxies, and they are used extensively in the automotive field, but, to the best of the authors' knowledge, no papers have as yet reported their use for braking systems. Several techniques for the adhesive joining of Carbon Fibre Reinforced Polymer (CFRP) to metals have been developed and reported in the literature, but only a few papers have reported the adhesive joining of CMC to metals [17].

In the present work, we have investigated and tested the adhesive joining of CMC to the EN AW 6082 Al alloy. An epoxy adhesive was chosen after a comprehensive and exhaustive bibliographic research activity, coupled with a screening of the commercially available products. The selected joining material is able to satisfy most of the requirements (high wettability and adhesion on both surfaces, i.e. of the CMC and the Al alloy, sound mechanical strength, easiness of manufacturing for large and complex areas, scalability to industrial components, and joining process at a lower temperature than 200°C) [18].

The novelty of this work concerns the functional design, manufacturing and characterisation of joints made between dissimilar materials (CMC and Al) that have to satisfy specific requirements imposed by the final application (the braking system).

## **2. Materials and methods**

The ceramic brake discs used in the experimental activity are based on a carbon short-fibre reinforced core material, which is exposed to liquid silicon infiltration, after the manufacturing of the green body and the pyrolysis process. An in situ reaction occurs between silicon and carbon and silicon carbide is formed; this results in a significantly lighter composite material than the cast iron used for conventional brake discs. The porosity remaining after the silicon infiltration ranges from between 0.5 and 3.0%.

At the end of the manufacturing process, the ceramic brake discs contain free silicon, silicon carbide and carbon, as both carbon fibre and residual pyrolytic carbon, in a 15-50-35% ratio. The bell disc is manufactured from the precipitation-hardened EN AW-6082 T6 Al alloy, which has a melting point of 585°C. The alloy is produced as an extruded bar, under a fully heat-treated condition (solution heat-treated and artificially aged) according to the T6 treatment; the bell disc is obtained from the processed bar. The composition of EN AW 6082 is in agreement with the UNI\_EN\_573-3 standard. An image of the BSCC ceramic composite brake is shown in Figure 1, while Figure 2 shows (a) the design of the standard braking system, which comprises a metallic bell connected to a CMC friction rotor by means of screws and nut bolts and (b) the new design of the brake, based on the bell joined, by means of adhesive, to the ceramic rotor, without any connecting elements. The experimental activity described in the present paper is related to the sketch shown in Figure 2 (b).

A joining material should be able to withstand processing temperatures of up to 200°C, in order to satisfy the two requirements described in the Introduction, and operating temperatures ranging from 100°C to 200 °C. The required shear strength of the joined component is about 25 MPa. This value represents the strength necessary for a braking system (metallic bell on the CMC disc) to operate under normal service conditions, and it is calculated on the basis of the shear stress generated in the lining material of the disc brake pad [18]. As shown in Figure 1, the joint is between two flat EN AW 6082 and CMC surfaces. For this reason, the experimental activity was carried out on rectangular-shaped (sandwich-like) samples.

## **2.1 Adhesive joining processing**

The CMC surfaces that had to be joined were polished with 800 grit paper and then ultrasonically cleaned in acetone for 5 min. The EN AW-6082 alloy surfaces were

blasted with  $\text{Al}_2\text{O}_3$  powder, using a sandblasting machine equipped with a pressure gauge to enable the desired power to be reached.

Subsequently, the metallic substrates were cleaned in an ultrasonic bath containing acetone.

The selected adhesive was a Supreme 42 HT-2 epoxy adhesive (SUP42 HT-2, Master Bond, The USA) and it was chosen to satisfy the requirements of the final component, for instance, sound mechanical strength and easiness of manufacturing, even for large components. The Supreme 42HT-2 adhesive has easy storage properties and a long shelf life, and is thus a promising candidate for industrial use.

According to the supplier's datasheets, the adhesive is a toughened sealant formulation that features excellent thermal cycling capabilities, high temperature resistance, high chemical resistance (good resistance to a wide range of chemicals, including many acids, bases, solvents, fuels and oils) and good flow properties. It is 100% solid, with completely reactive formulations, and shows low shrinkage upon curing.

The Supreme 42HT-2 adhesive is a bi-component epoxy adhesive (mix ratio of 100 to 40 by weight or 100 to 50 by volume). Supreme 42HT-2 has a large service temperature range ( $-62^\circ\text{C}$  to  $230^\circ\text{C}$ ) and is compatible with the final service application of an Al alloy/CMC joined component. Moreover, it has high thermal conductivity and a low thermal expansion coefficient ( $34 \cdot 10^{-6} \text{ K}^{-1}$ ), compared to other structural adhesives, as well as good adhesive properties on both the ceramic and metallic surfaces, and it shows a noteworthy capacity to resist thermal cycling [19]. According to the supplier's datasheet, curing can be carried out at room temperature for 48-72 hours or at  $94^\circ\text{C}$  for 2-3 hours, but the recommended curing schedule to obtain optimal properties is 12 hours at room temperature, followed by 3-5 hours at  $72-94^\circ\text{C}$ .

In order to find the best curing process for this application, Supreme 42HT-2 was cured in a slightly different way from the cure schedule suggested by the supplier, conducting

two different thermal treatments. Both treatments were chosen after a thermal analysis (discussed hereafter) on the adhesive, starting from the supplier's specifications. In the first thermal treatment, the curing parameter was set at room temperature for 12 hours and this was followed by 5 hours at 90°C. The second treatment involved two steps: the first one was the same as the previous one (at room temperature for 12 hours followed by 5 hours at 90°C), but the second step consisting of a thermal ageing of 10 minutes at 200°C.

The adhesive was applied to the facing surfaces using a spatula; a sufficient amount of mixed adhesive was applied to obtain a final adhesive bondline with a suitable thickness. The CMC surface was rather dense, and it permitted the same amount of adhesive required for the denser metallic surface to be used (no additional adhesive was required to fill the voids that occurred naturally as texturing results of CMC).

A weight of about 80 g, corresponding to a pressure of about 1 kPa, was placed on the top of sandwiched samples to keep them in place.

The EN AW 6082 samples were used under two different conditions: with an anodised surface and “as received”, i.e. without any anodised surface. The anodisation treatment is a chemical process; the Al alloy bell is anodised to create a thick (about 35 microns), hard coating on the bell housing to increase hardness and durability. This process leads to a coating that is formed by a porous anodic oxide filled with a corrosion inhibited organic primer; in addition, organic pigments are utilised to achieve the dark colour of the Al bell.

In the following description, the EN AW 6082 samples refer to uncoated surfaces (i.e. no anodisation treatment was performed on EN AW-6082), unless otherwise indicated. A sandblasting treatment was only carried out on uncoated samples.



The curing cycles for the different adhesives were conducted in air inside an oven (Binder GmbH, Tuttlingen, Germany). The samples were introduced directly into the furnace at the treatment temperature and then left to cool slowly to room temperature.

## **2.2 Material Characterisation**

The epoxy curing conditions were evaluated by means of Differential Scanning Calorimetry (DSC), (Mettler Toledo, Star system DSC 1, USA). Samples with masses of approximately 10 mg were cured in aluminium pans with pierced lids in a nitrogen atmosphere. DSC was used to study non-isothermal curing at a heating rate of 5 °C/min up to 250 °C in order to evaluate the heat release at total conversion; isothermal curing was then evaluated at 80 and 90 °C to measure the conversion of the epoxy group during curing. The data were analysed by means of Mettler Toledo STARe software, V9.2.

A dynamic thermal-mechanical analysis (DMTA) was performed using a Triton Technology instrument. The following parameters were considered: a 3 °C/min heating rate, a 1 Hz applied tensile stress and a strain of 0.02%. The measured samples had average dimensions of 12 mm x 8 mm x 0.8. mm.

The CMCs and EN AW 6082 were both sliced into rectangular 25 mm × 25 mm × 6 mm pieces (bonding surface: 25 mm × 12.5 mm, half overlapping) for the joining process tests to match the shear test set-up.

The mechanical strength (apparent shear strength) of the joined samples was determined using a single lap offset (SLO) test, under compression, using a method adapted from the ASTM D1002-05 standard (universal testing machine SINTEC D/10) [20].

The test configuration and the geometry of the fixture are reported in [21]. The load was applied to the metallic part of the joint by moving the cross-head at a speed of 1 mm/min (Figure 3); the apparent shear strength was calculated by dividing the

maximum recorded force by the joining area. At least 7 samples were tested for each joint. All the fracture surfaces were observed and macroscopically characterised according to DIN EN ISO 10365 [22]. The results of the mechanical tests were expressed as mean  $\pm$  standard deviation.

The joined samples were tested, after thermal cycling, to obtain a preliminary screening of the thermal performance of the joints; thermal cycling was carried out at 200°C for 10 minutes and the soundness of the samples was tested, by means of a SLO test, after 1, 5 or 10 cycles.

The joining materials and joints were also submitted to a salt spray test, according to ISO 9227, for 240 h and 720 h. The saline mist tests were carried out at the Brembo SGL Carbon Ceramic Brakes (BSCCB) facilities in Stezzano-BG (Italy).

Cross-sections of the joints were investigated, before and after the saline mist test and thermal cycling, while the fracture surfaces were investigated, after lap-shear tests, by means of Field Emission Scanning Electron Microscopy, equipped with Energy Dispersive Spectroscopy (FESEM-EDS SUPRATM 40, Zeiss and Merlin Gemini Zeiss).

### **3. Results and discussion**

The epoxy adhesive selected in order to guarantee the widest possible range of properties and to be the most suitable joining material for the substrates investigated in the present work.

It was selected and tested to fulfil the requirement established by the end-user, according to the criteria reported in the Introduction section, i.e. the maximum joining process temperature had to be lower than 200°C, in order to avoid compromising the mechanical properties of EN AW 6082. Galvanic corrosion resistance was not considered for the selection of the joining materials in this work. However, it was

necessary to exclude metallic brazes from the selection of the viable joining materials, since a brazed seam can represent a weak point of a joined component, as metals are susceptible to corrosion from road salt, dirt and water. However, this is not an issue for polymeric adhesives. Furthermore, the relatively low temperature requested for the joining process rules out brazing alloys as suitable joining materials.

The surface finishing of the metallic part of the joint, i.e. EN AW 6082, is connected to the brake disc application context. Aluminium bells for brake systems are usually supplied without any specific surface treatment, because they do not need to fulfil any specific corrosion requirements; however, an additional anodisation treatment is required for the Al brakes of higher-quality vehicles to increase the protection against corrosion and wear resistance, and to improve their appearance. The joined braking system discussed in the present paper is usually manufactured using a non-anodised aluminium belt coupled with a CMC rotor.

### **3.1 Joining with the Supreme 42 HT-2 epoxy adhesive**

The performance of a joint manufactured using a polymeric adhesive is often associated with effective/ineffective curing process parameters; the curing process needs to be monitored and controlled precisely in order to improve the quality of the joints and, as a consequence, their durability and mechanical performances. In the present work, the activity was aimed at investigating the optimised curing process (temperature and time) to prevent the worst case scenarios, i.e. under-curing and premature demoulding, which can result in severe effects on the performance of a joint.

As a first step, DSC-dynamic analyses were performed to evaluate the best curing conditions. The area underneath the exothermic peak can be used to determine the conversion of the epoxy group upon curing. The DSC-dynamic curve of the 42 HT-2 epoxy resin is shown in Figure 4. An exothermic peak can be observed at around 90°C

and a total exothermicity of 198.77 J/g, attributable to the conversion of the total epoxy group upon curing, was measured. Therefore, the epoxy curing process was studied at around this temperature, in order to evaluate the reaction time.

DSC-isothermal analyses were carried out at 80 °C and 90 °C. Figure 5 shows the DSC-isothermal curves of the samples cured at different temperatures. A reaction exothermicity of 100.39 J/g, which corresponds to an epoxy group conversion of 50%, was recorded at 80 °C, and an exothermicity of 118.45 J/g, corresponding to an epoxy group conversion of about 60%, was recorded at 90 °C.

As expected, a higher conversion was obtained at the higher temperature, since there is a delay in vitrification, and the reaction reached vitrification within 5 hours at both temperatures. The glass transition temperature ( $T_g$ ) of the epoxy material, crosslinked at 90 °C for 5 hours, was around 73 °C, as measured by means of DMTA analysis. The  $E'$  storage modulus and  $\tan\delta$  curves recorded for the crosslinked epoxy adhesive are reported in Figure 6.

According to the curing conditions evaluated by means of DSC analysis, the joining process consisted of 12 hours of curing at ambient temperature, followed by a post cure at 90°C for 5 hours; this procedure is hereafter referred to as “standard process”.

The aim of the thermal investigation was to detect and reach the highest possible conversion before vitrification. The curing process for the adhesive corresponds to the joining process: during curing, the epoxy group starts a polymerisation reaction, which in turn leads to cross-linking and hardening. This process has a marked impact on the adhesion of the joining material on the surfaces that have to be joined.

Cross-sections of CMC joined to EN AW 6082 with the SUP42 HT-2 epoxy adhesive are shown in Figure 7. The bonding layer is about 150  $\mu\text{m}$  thick, uniform and dense, and the interfaces are continuous, without cracks or pores, which indicates that the joint has the potential to exhibit high bonding strength. Good adhesion of the joining material

with both surfaces (CMC and EN AW 6082) can be observed in all the joints; the composite/adhesive interface (red arrows in Figure 7b) shows an interlocked surface at a higher magnification, due to the flow of the adhesive and its penetration of the composite fabric and of the porosities of the composite all along the irregular fibre surface.

Regarding the interface between the adhesive and the EN AW-6082, the grit-blasting process was successful in roughening the metallic surface, thus increasing the effective bonding area. This enhanced surface roughness was expected to increase the adhesion of the joining material and increase the bonding strength.

A surface treatment of adherends usually results in improved adhesive joint shear strength. Several studies have reported the use of metallic surface treatment methods (such as mechanical abrasion, grit blasting or sandblasting) before performing joining processes; the most frequently studied metallic substrates are steel and aluminium alloys [23, 24]. For example, grit blasting causes a noteworthy enhancement of the joint strength on aluminium surfaces [25]. Surface treatments are able to improve the adhesion between a substrate and an adhesive by increasing the interfacial bond area as a result of the higher surface roughness and mechanical interlocking caused by surface texturing [26, 27].

A similar thermal cycling process to the one normally conducted in braking systems (1, 5 or 10 cycles at 200°C for 10 minutes) was performed on samples joined using the standard process (12 hours at ambient temperature, followed by a post cure at 90°C for 5 hours) to assess the reliability of these joints under service conditions.

Thermal cycling may generate stresses in bonded components: due to the thermal expansion mismatch of the adherends, thermal cycling may generate even higher stresses in dissimilar joints. Such stresses can initiate critical cracks in the joined region, which can propagate, thus reducing the strength of the joints under working conditions.

All the joined samples were tested by means of a single-lap offset test under compression; the average (apparent) shear strength is reported in Table 1. The joined samples obtained using the standard joining process exhibit a mechanical strength of  $31.6 \pm 7.2$  MPa. The results of the mechanical tests carried out on joined samples after 1, 5 or 10 cycles show that the average shear strength of the samples thermally cycled once or five times is almost identical, while the mechanical strength is higher in the case of joined samples after 10 cycles. This could be due to a further advancement of the curing reaction during each thermal cycle, which induced a further enhancement of the crosslinking density.

The better behaviour of the 10-cycle tested samples could be explained by considering a thermal effect that was further activated during the curing reactions and which increased the intrinsic adhesive strength.

As a consequence of this increase in mechanical strength, the effect of a fast post-thermal treatment on the cured joints was evaluated by heating the joined samples at 200 °C for 10 minutes (which is comparable to 10 thermal cycles at 200°C for 1 minute). Complete conversion should be reached in the epoxy joint as a result of such a fast temperature treatment, as a very high crosslinking density is achieved.

The morphological analysis of an EN AW 6082 alloy joined to CMC with SUP42 HT-2, using a post thermal treatment at 200 °C for 10 minutes, displays the same features as the cross-section of the samples processed by means of the standard joining process (Figure 8). Both joint interfaces are microstructurally sound, without cracks or voids, and the infiltration of the adhesive into the composite fabric is still observable. Again, in this case, as in the joints obtained by means of the standard joining process ( i.e. 12 hours at room temperature and curing at 90 °C for 5 hours), no pores are observable in the middle of the joint area, thus indicating that no bubbles, originating from entrapped air during the curing process, are present in the joints. Such bubbles could be

detrimental to the mechanical resistance of the joints, since they can act as the starting points of cracks.

As far as the mechanical characterisation is concerned, the samples manufactured with a post thermal treatment at 200 °C for 10 minutes show a value of  $38.2 \pm 6.4$  MPa (Table I). Comparing this average value with that of the samples obtained by means of the standard joining process, it may be observed that the mechanical strength of the thermally treated joints increases by about 21%. This may be due to the higher epoxy group conversion reached during the thermal post-treatment, which results in a higher crosslinking and therefore a higher mechanical performance of the adhesive.

The typical load/displacement curve of the CMC/ EN AW 6082 joints, as tested by means of SLO, shows brittle behaviour. Figure 9 shows, as an example, the load/displacement curves of a joined CMC/ EN AW 6082 sample, manufactured using SUP 42 HT-2, by means of the standard joining process.

As a final consideration about the mechanical characterisation of the joints, it was found that the bonding strength was higher than the required value (25 MPa) for all the tested samples.

The EN AW 6082 /CMC joint samples were also submitted to salt spray tests for 240 or 720 hours. Exposure to a salt spray for a long period of time can induce corrosion of the metallic parts of brake components, as well as corrosion or degradation of the joined area. From the morphological point of view (Figure 10), no significant changes were detected in the joint areas, compared to the non-salt sprayed samples, while a noteworthy degradation was observed on the EN AW 6082 free surface (i.e. the surface exposed to the environment, and not the one facing directly onto the CMC part), as shown in Figure 11. The mechanical performance of the samples exposed to a salt spray and the average shear strength values are summarised in Table I and in Figure 12. The mechanical strength is significantly reduced, compared to the non-salt sprayed samples,

but no statistically significant difference can be observed between the shorter tests (240 h) and the longer ones (720 h). It is worth noting that the shear strength threshold value of the joints (25 MPa) has not been reached for the samples submitted to the salt spray test.

However, this result can be considered acceptable as a first approximation: the samples were submitted to the salt spray test for a much longer period of time than 96 hours, the duration recommended in the ISO 27667:2011 International Standard [28] and, in most cases, cars using these brake systems are hardly ever used under such severe conditions for longer than the 240 hours in the corrosive environment of the salt spray test.

However, artificial exposure might not necessarily have the same effects as natural exposure; field-testing should be adopted to assess the corrosion resistance of the brake system, in order to provide comprehensive information on the life cycle of these components.

Some joined EN AW 6082 /CMC samples were manufactured using anodised EN AW 6082 substrates and the same joining material, i.e. SUP 42 HT-2. The shear strength values of these joints are summarised in Figure 12. The measured values of the anodised samples are slightly lower than those measured for non-anodised EN AW 6082, although they are statistically comparable with each other.

However, the coating on the metallic substrate has a detrimental effect on the adhesion of the adhesive whenever a thermal post-treatment is applied, and this leads to a dramatic decrease in the shear strength (Table I and Figure 12). It should be recalled, as previously mentioned, that the metallic part of the joint was not sandblasted in order to preserve the coating.

Figure 13 shows the fracture surfaces of some representative mechanically tested joints; failure occurred adhesively at the adhesive/CMC interface, or within the composite, for



all the samples, thus indicating a stronger interface between the epoxy resin and the metallic substrate.

This behaviour has also been observed for samples submitted to salt spray tests. It is known that Al alloys generate shallow pitting corrosion after salt spray tests, but, in our case, the EN AW 6082 surface was protected by the joining material, at least in the joint area. The fracture surfaces are similar for all the tested samples, with the exception of the anodised samples, regardless of the thermal/ageing treatment applied (standard joined, thermally cycled or tested under a salt spray). The fracture surfaces of the anodised EN AW 6082 /CMC joints (Figure 13) clearly show that the failure occurred at the anodised surface/adhesive interface, thus demonstrating that anodisation of the surface is detrimental for the adhesion of this joining material, at least in the case of optimised adhesive curing (i.e. post-treatment at 200°C). The failure pattern of the bonded assemblies, based on the anodised metallic parts, confirms the low mechanical resistance of these samples, as reported in Table 1.

A morphological analysis of all the fracture surfaces was carried out by means of SEM. The fracture surface analysis showed that cracks occurred inside the composite and/or at the adhesive/CMC interface. Figures 14 and 15 show typical fracture surfaces of an EN AW 6082 /CMC joined sample, manufactured using a post-treatment at 200°C for 10 minutes: the presence of the composite is evident on both sides (Figure 14: EN AW 6082 side, Figure 15: CMC side). The fracture mechanism in Figures 14 (b) and 14 (c) shows fibre failure, while the presence of pure Si (white areas) is clearly visible in other fracture surface regions. Furthermore, the EDS analysis revealed the presence of carbon and silicon on both fracture surfaces, thus confirming that failure did not occur within the adhesive but rather at the CMC/adhesive interface or just underneath the CMC surface, and that the joint strength is higher than the interlaminar shear strength of the

composite itself. Delamination of the composite is clearly visible in some areas on the fracture surfaces (Figures 15 (a) and 15 (b)).

A hypothesis of the crack path is reported in Figure 16, which also shows a possible failure pattern, based on a visual inspection of the tested samples. However, such a pattern would not be observed in the case of anodised Al alloy adherends.

For the sake of completeness, thermally cycled fracture surface samples and samples after the salt spray test are shown in Figures 17, 18 and 19. The corrosion effect on the metallic part is clearly visible on the fracture surfaces of the mechanically tested joints after the salt spray tests (Figure 18 (a) and Figures 19 (b) and (c)). The Al alloy is susceptible to a localised corrosion process, whenever it is exposed to a saline environment: some corrosion products are detectable on the EN AW 6082 surface (Figure 11). The metallic surface in the joint area is protected by the adhesive; accordingly, the fracture path, after the mechanical test, does not appear to be so different for the saline tested samples and the samples not submitted to salt spray tests.

## **Conclusions**

The requirements that arise from the design and performance of a vehicle have an important effect on the selection of the used materials; this is especially true for ceramic composite brake discs, which are frequently used in sports cars, high-powered luxury sedans and SUVs.

Accurate knowledge of the manufacturing routes and the joining process used to connect specific parts is necessary for a successful development of a product.

The activity presented in this paper falls into this context; the use of an epoxy resin (SUP 42-HT) to join CMC composites to an Al alloy (EN AW 6082) is reviewed and discussed.

This study has shown that a proper balancing between an enhanced roughness of the metal surface and the optimisation of the adhesive curing process has an important impact on the epoxy.

The chosen epoxy resin (SUP 42-HT) was effective in joining CMC to sand-blasted or anodised EN AW 6082, and the bonding strength of the joints fulfilled the minimum shear strength requirements. The performed thermal cycles did not affect the mechanical properties of these joints or their failure propagation mode to any great extent.

Moreover, a reduction in the average mechanical strength was observed for the samples submitted to the salt spray test, thus showing that a corrosive environment can affect adhesive joined brake components.

The relevance of the findings obtained from the experimental activity goes beyond the specific application of the investigated epoxy resin. The effect of the curing on the performance of the adhesive has been studied; the higher epoxy group conversion reached during the thermal post-treatment of the adhesive leads to an improved mechanical strength of the joints.

## **Acknowledgements**

The authors would like to thank Dr Marco Nagliati for his collaboration and the helpful discussion.

## **References**

- [1] N. Langhof, M. Rabenstein, J. Rosenlöcher, R. Hackenschmidt, W. Krenkel, F. Rieg, Full-ceramic brake systems for high performance friction application, J. Eur. Cer. Soc. 36 (2016): 3823–3832. <https://doi.org/10.1016/j.jeurceramsoc.2016.04.040>

- [2] L. Wanyang, Y. Xuefeng, W. Shouren, X. Jupeng, H. Qimin, Research and prospect of ceramics for automotive disc-brakes, *Ceram. Int.* 47, 8 (2021) : 10442-10463. [https://doi.org/ 10.1016/j.ceramint.2020.12.206](https://doi.org/10.1016/j.ceramint.2020.12.206)
- [3] R. Renz , G. Seifert, W. Krenkel, Integration of CMC Brake Disks in Automotive Brake Systems, *J. Appl. Ceram. Technol.* 9, 4 (2012): 712–724. <https://doi.org/10.1111/j.1744-7402.2012.02812.x>
- [4] D. Alei, L. Tiehu, W. Jianqing, Z. Tingkai, X. Yu, C. Xudong, L. Hao, T. Chen, X. Chuanyin, Preparation and mechanical properties of CCF reinforced RBSC braking composite from pre-liquid dispersion, *Ceram. Int.* 45, 5 (2019): 6528-6534. <https://doi.org/>
- [5] F. Shangwu, Z. Litong, C. Laifei, Y. Shangjie, Microstructure and frictional properties of C/SiC brake materials with sandwich structure, *Ceram. Int.* 37 (2011) : 2829-2835. [https://doi.org/ 10.1016/j.ceramint.2018.12.145](https://doi.org/10.1016/j.ceramint.2018.12.145)
- [6] X. Yongdong, Z. Yani, C. Laifei, Z. Litong, L. Jianjun, Z. Junzhan, Preparation and friction behavior of carbon fiber reinforced silicon carbide matrix composites, *Ceram. Int.* 33, 3 (2007): 439-445. [https://doi.org/ 10.1016/j.ceramint.2005.10.008](https://doi.org/10.1016/j.ceramint.2005.10.008).
- [7] Z. Li, P. Xiao, B.G. Zhang, Y. Li, Y.H. Lu, Preparation and tribological properties of C/C–SiC brake composites modified by in situ grown carbon nanofibers, *Ceram. Int.* 41, 9 Part B (2015): 11733-11740. [https://doi.org/ 10.1016/j.ceramint.2015.05.139](https://doi.org/10.1016/j.ceramint.2015.05.139).
- [8] R. Asim, Overview of Disc Brakes and Related Phenomena - a review. *Int. J. Vehicle Noise and Vibration*, 10, 4 (2014): 257- 301. [https://doi.org/ 10.1504/IJVNV.2014.065634](https://doi.org/10.1504/IJVNV.2014.065634)

- [9] S. M. Sapuan, Concurrent Engineering in Design and Development of Composite Products In: Composite Materials Concurrent Engineering Approach. Amsterdam: Elsevier, 2017. pp 95-139.
- [10] G. Mrówka, J. Sieniawski, A. Nowotnik, Effect of heat treatment on tensile and fracture toughness properties of 6082 alloy, J. Ach. Mat. Manufact. Eng. 32, 2 (2009): 162-170. <https://doi.org/>
- [11] C. Yigao, C. Yejie. W. Yiguang, Electrical property of joints made of polymer-derived SiAlCN ceramic via adhesive joining, Ceram. Int. 47, 3 (2021) : 3649-3656. [https://doi.org/ 10.1016/j.ceramint.2020.09.216](https://doi.org/10.1016/j.ceramint.2020.09.216).
- [12] W. Mingchao, L. Jiachen, D. Haiyan, H. Feng, G. Anran, L. Shan, D. Xue, Joining of C/C composites by using B4C reinforced phosphate adhesive, Ceram. Int. 40, 8 Part A (2014): 11581-11591. [https://doi.org/ 10.1016/j.ceramint.2014.03.123](https://doi.org/10.1016/j.ceramint.2014.03.123).
- [13] W. Xiaozhou, W. Jun, W. Hao, Preparation of high-temperature organic adhesives and their performance for joining SiC ceramic, Ceram. Int. 39, 2 (2013): 1365-1370. [https://doi.org/ 10.1016/j.ceramint.2012.07.075](https://doi.org/10.1016/j.ceramint.2012.07.075).
- [14] F. Cavezza, M. Boehm, H. Terryn, T. Hauffman, A Review on Adhesively Bonded Aluminium Joints in the Automotive Industry, Metals 10 (2020) : 730. [https://doi.org/ 10.3390/met10060730](https://doi.org/10.3390/met10060730)
- [15] T. Barnes, I. Pashby. Joining techniques for aluminium spaceframes used in automobiles. J. Mater. Process. Technol. 99 (2002): 72–79. [https://doi.org/ 10.1016/S0924-0136\(99\)00361-1](https://doi.org/10.1016/S0924-0136(99)00361-1)
- [16] A. Pramanik, A.K. Basak, Y. Dong, P. K. Sarker, M. S. Uddin, G. Littlefair, A. R. Dixit, S. Chattopadhyaya, Joining of carbon fibre reinforced polymer (CFRP) composites and aluminium alloys – A review. Compos. Part A-Appl. S. 101 (2017): 1-29. <https://doi.org/10.1016/j.compositesa.2017.06.007>

- [17] M. Salvo, V. Casalegno, M. Suess, L. Gozzelino, C. Wilhelmi, Laser surface nanostructuring for reliable Si<sub>3</sub>N<sub>4</sub>/Si<sub>3</sub>N<sub>4</sub> and Si<sub>3</sub>N<sub>4</sub>/Invar joined components, *Ceram. Int.* 44 (2018) : 12081–12087.  
<https://doi.org/10.1016/j.ceramint.2018.03.226>.
- [18] Private communication, BSCCB-Brembo SGL Carbon, May 2020
- [19] Masterbond datasheet; <https://www.masterbond.com/tds/supreme-42ht-2>
- [20] ASTM D1002-05. Standard Test Method for Apparent Shear Strength of Single-Lap-Joint Adhesively Bonded Metal Specimens by Tension Loading (Metal-to-Metal), 2005
- [21] M. Suess, C. Wilhelmi, M. Salvo, V. Casalegno, P. Tatarko, M. Funke, Effect of pulsed laser irradiation on the SiC surface, *Int. J. Appl. Ceram. Technol.* 14 (2017): 313–322. <https://doi.org/10.1111/ijac.12655>.
- [22] ISO 10365 standard. Adhesives – Designation of Main Failure Patterns, 1992.
- [23] J.P.B. van Dam, S.T. Abrahams, A. Yilmaz, Y. Gonzalez-Garcia, H. Terryn, J.M.C. Mol, Effect of surface roughness and chemistry on the adhesion and durability of a steel-epoxy adhesive interface. *Int. J. Adhes. Adhes.* 96 (2020) 102450. <https://doi.org/10.1016/j.ijadhadh.2019.102450>.
- [24] A.M. Pereira, J.M. Ferreira, F.V. Antunes, P.J. Bártolo Analysis of manufacturing parameters on the shear strength of aluminium adhesive single-lap joints, *J. Mater. Process. Tech.* 210 (2010) 610–617.  
<https://doi.org/10.1016/j.jmatprotec.2009.11.006>.
- [25] S. Azari, M. Papini & J. K. Spelt, Effect of Surface Roughness on the Performance of Adhesive Joints Under Static and Cyclic Loading. *The Journal of Adhesion*, 86:7, 742-764 <https://doi.org/10.1080/00218464.2010.482430>
- [26] T. Kleffel, D. Drummer, Investigating the suitability of roughness parameters to assess the bond strength of polymer-metal hybrid structures with mechanical

adhesion. *Compos. Part B Eng.* 117 (2017) 20- 25.

<https://dx.doi.org/10.1016/j.compositesb.2017.02.042>

[27] S.Budhe, A. Ghumatkar, N. Birajdar, M. D. Banea. Effect of surface roughness using different adherend materials on the adhesive bond strength. *Appl. Adhes. Sci.* (2015) 3:20. <https://doi.org/10.1186/s40563-015-0050-4>

[28] International Standard ISO 27667:2011- Road vehicles — Brake lining friction materials — Evaluation of corrosion effects on painted backing plates and brake shoes

### **Figure captions**

**Figure 1.** A BSCC ceramic composite brake with a CMC friction rotor and Al alloy bell

**Figure 2.** Cross-section showing the geometry of the brake disc with (a) the standard joined component, i.e. the bell connected to the CMC friction rotor by means of screws and nut bolts (a) and the new design of the brake, without any connecting elements and a joined area (red line) (b).

**Figure 3.** Test configuration and geometry of a joined specimen for the single lap offset test under compression.

**Figure 4.** A DSC curve of the SUP 42 –HT epoxy resin obtained from a 5°C/min scan

**Figure 5.** DSC isothermal scans of the SUP 42 –HT epoxy resin at 80°C (a) and at 90°C (b)

**Figure 6.** DMTA analysis of the thermally cured SUP42 HT-2 epoxy adhesive

**Figure 7.** Optical cross-section micrographs of the CMC/ EN AW 6082 joints bonded by SUP42 HT-2 (a); magnification of the interface between the adhesive and the ceramic part of the joint (b)

**Figure 8.** SEM cross-section micrographs of (a) CMC/ EN AW 6082 joints (adhesive curing using a post thermal treatment at 200 °C for 10 minutes) bonded with SUP42 HT-2 and (b) magnification of the interface

**Figure 9.** Load/displacement curve of a CMC/ EN AW 6082 joint manufactured using SUP42 HT-2 by means of the standard joining process

**Figure 10.** SEM microscopy (a) of the cross-section of the CMC/ EN AW 6082 joint after the 240 h salt spray test; magnification of the adhesive/Al interface (b) and of the CMC/adhesive interface (c)

**Figure 11.** Top view SEM magnification of an EN AW 6082 part after the 240 h salt spray test; the image refers to an Al alloy area outside the joint

**Figure 12.** Results of the mechanical tests. Legend: ST = standard treatment, PT = post-treatment at 200 °C/10 min, TA = thermal ageing at 200 °C (each cycle 1 min), SST = salt spraying tests.

**Figure 13.** Fracture surfaces of Al alloy/CMC samples joined with SUP 42 HT-2 after the SLO shear test (EN AW 6082 surface on the left and CMC surface on the right for each surface macrography)

**Figure 14.** SEM images of fracture surfaces of the CMC / EN AW 6082 joints (adhesive curing with a post-treatment at 200°C for 10 minutes) (Al alloy side) after the SLO shear test

**Figure 15.** SEM images of fracture surfaces of the CMC / EN AW 6082 joints (adhesive curing with a post-treatment at 200°C for 10 minutes) ( CMC side) after the SLO shear test; delamination of the composite is detectable

**Figure 16.** A schematic of a possible fracture path in EN AW 6082 /CMC joints (but not for an anodised sample)

**Figure 17.** SEM images of fracture surfaces of the tested joints after 10 cycles at 200°C and the SLO shear test



**Figure 18.** SEM images of fracture surfaces of the tested joints after the 240 h salt spray test and SLO shear test

**Figure 19.** SEM images of fracture surfaces of the tested joints after the 720 h salt spray test and SLO shear test; a compositional analysis of some areas is reported in the insets (Cr detection is due to metallisation of the samples with a conductive Cr layer)

		Standard joining process	Post thermal treatment 200°C/10 min	1 thermal cycle (200°C/1 min)	5 thermal cycles (200°C/1 min)	10 thermal cycles (200°C/1 min)	Salt spray test 240 h	Salt spray test 720 h
Al alloy/CMC joint	Average shear strength [MPa]	31.6	38.2	27.3	29.3	35.4	18.7	15.1
	dev st [MPa]	7.2	6.4	4.8	2.7	8.1	3.2	8.2
Anodised Al alloy/CMC joint	Average shear strength [MPa]	27.6	6.9					
	dev st [MPa]	7.5	2.1					

**Table 1** Summary of the SLO mechanical test results on the SUP 42HT-2 joined EN AW 6082 /CMC samples manufactured using several curing treatments, after thermal cycling and after the salt spray test

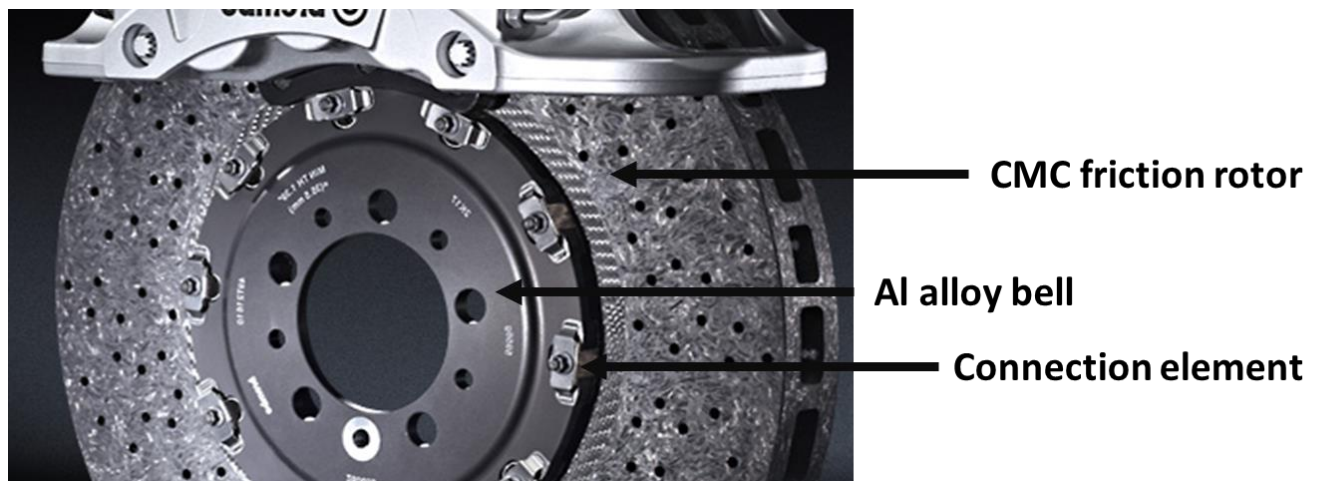


**Figure 1** BSCC ceramic composite brake with a CMC friction rotor and Al alloy bell

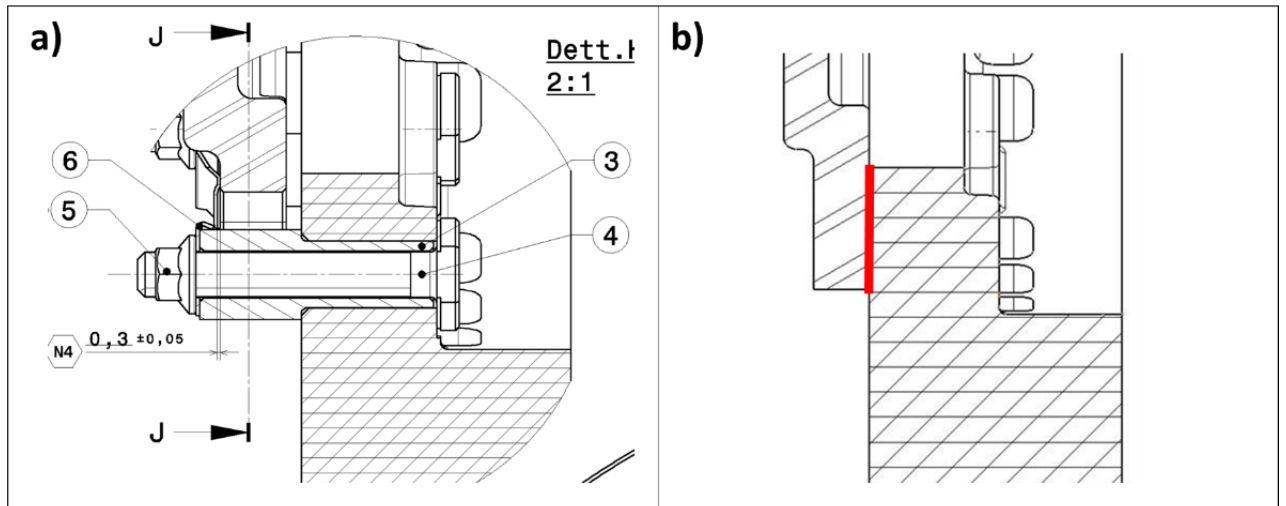


**Figure 2** Cross-section showing the geometry of the brake disc with (a) the standard joined component, i.e. the bell connected to the CMC friction rotor by means of screws and nut bolts (a) and the new design of the brake, without any connecting elements and a joined area (red line) (b).

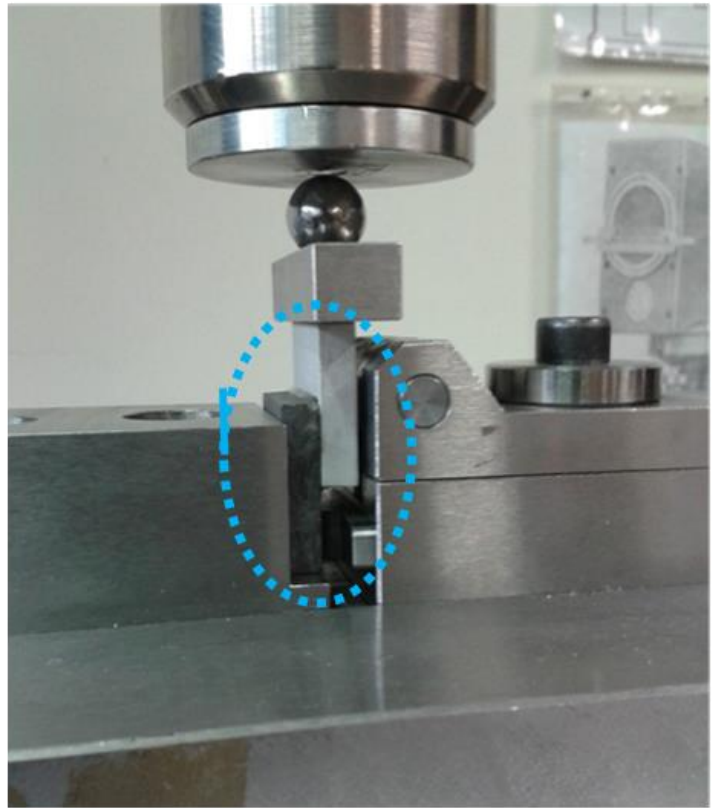
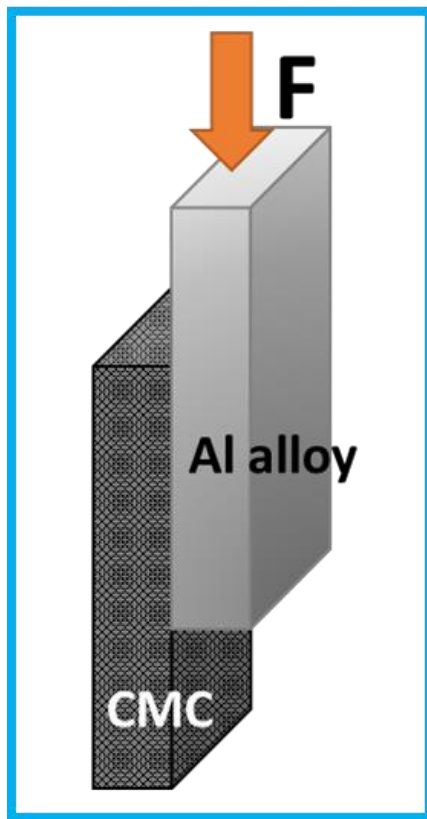


**Figure 3** Test configuration and geometry of a joined specimen for the single lap offset test under compression.

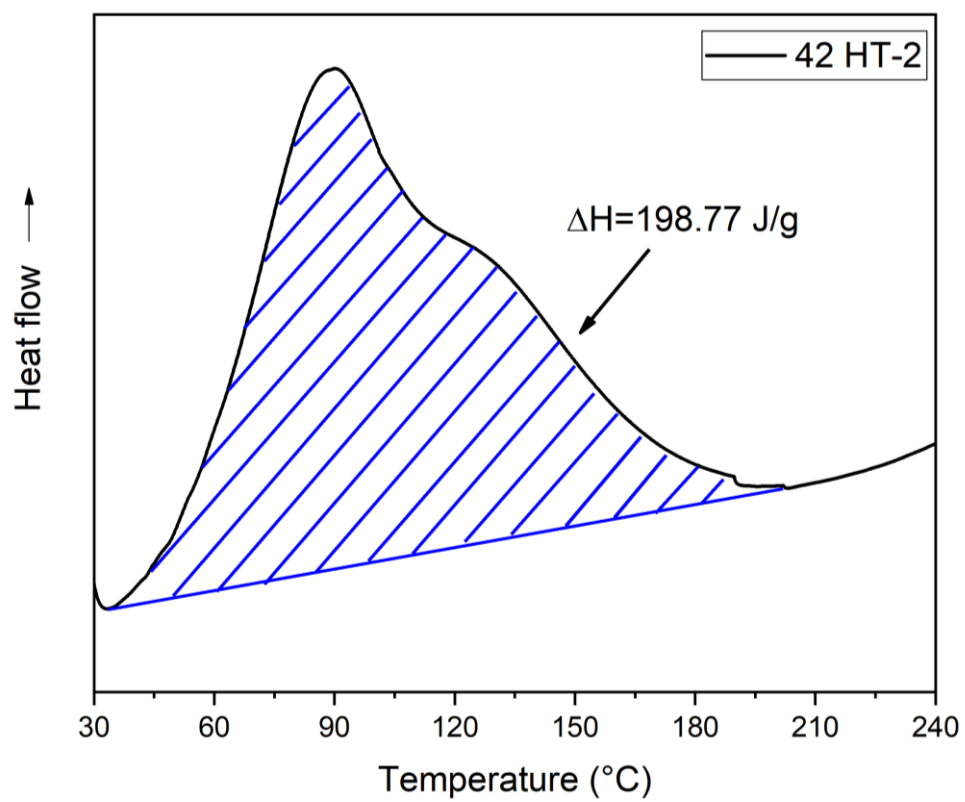


**Figure 4** DSC curve of t SUP 42 -HT epoxy resin\_obtained from a 5°C/min scan

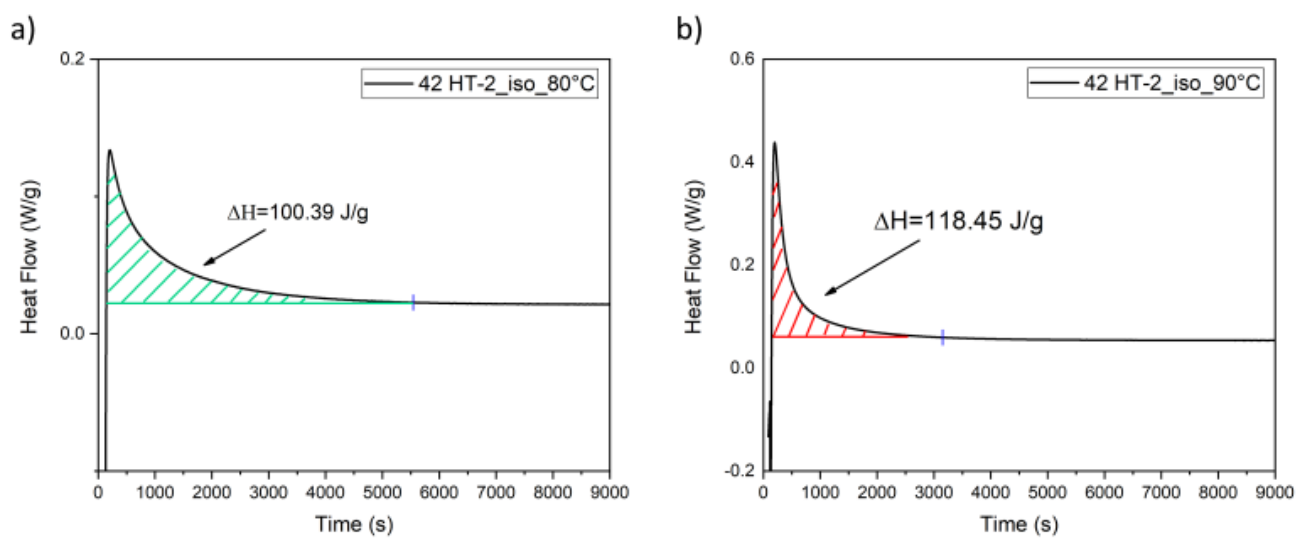


**Figure 5** DSC isothermal scan of the SUP 42 –HT epoxy resin at 80°C (a) and at 90°C

(b)

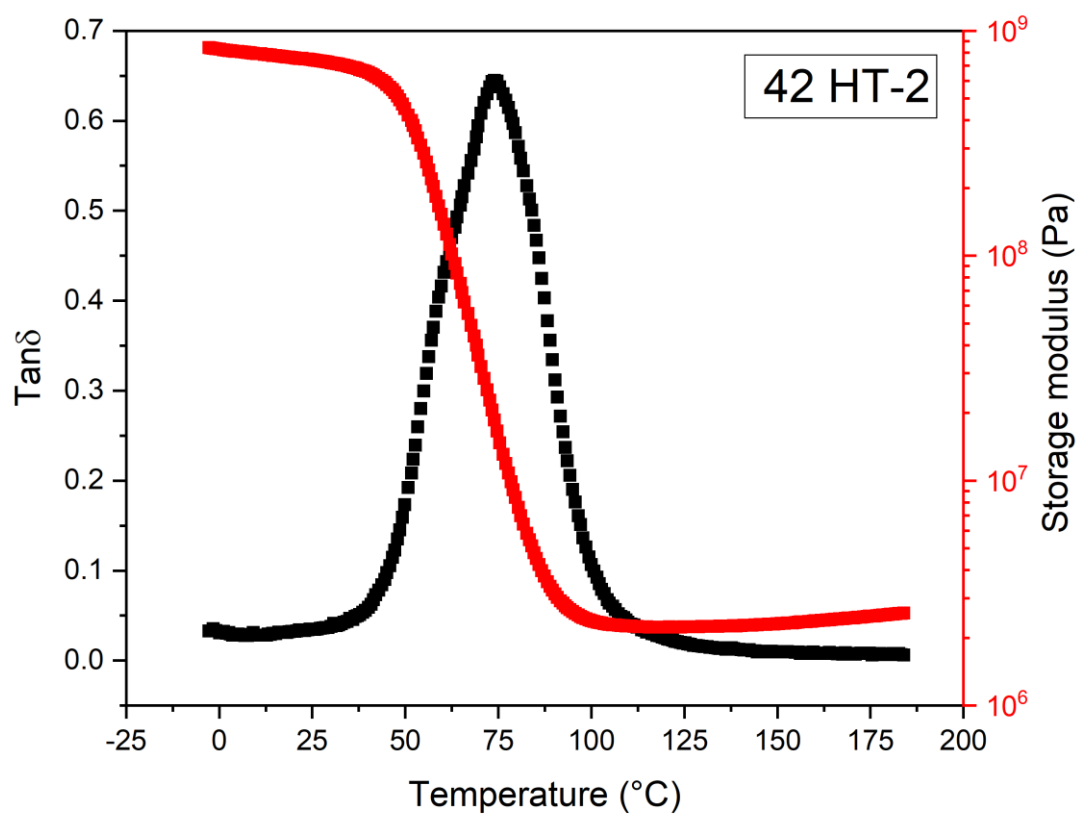


**Figure 6** DMTA analysis of the thermally cured SUP42 HT-2 epoxy adhesive



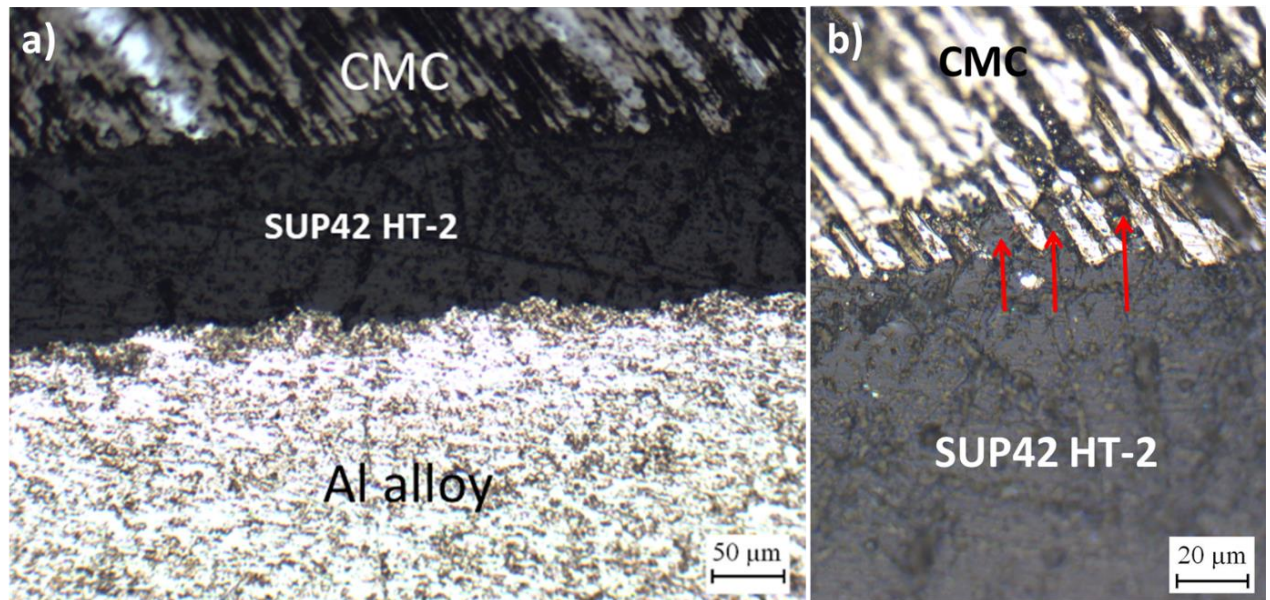


**Figure 7** Optical cross-section micrographs of the CMC/ EN AW 6082 joints bonded by SUP42 HT-2 (a) ; magnification of the interface between the adhesive and the ceramic part of the joint (b)

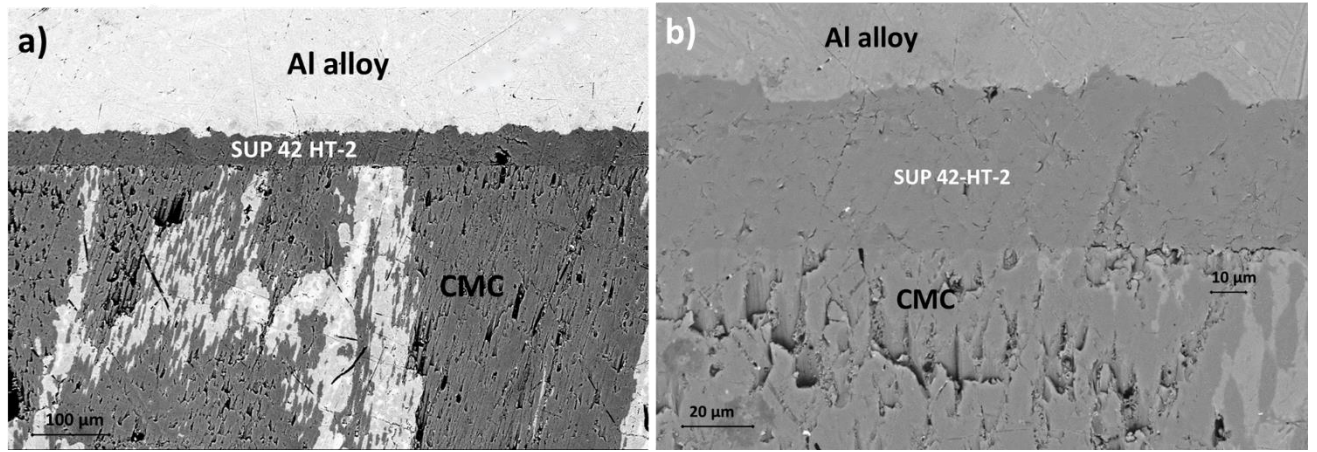


**Figure 8** SEM cross-section micrographs of (a) CMC/ EN AW 6082 joints (adhesive curing using a post thermal treatment at 200 °C for 10 minutes) bonded with SUP42 HT-2 and (b) magnification of the interface

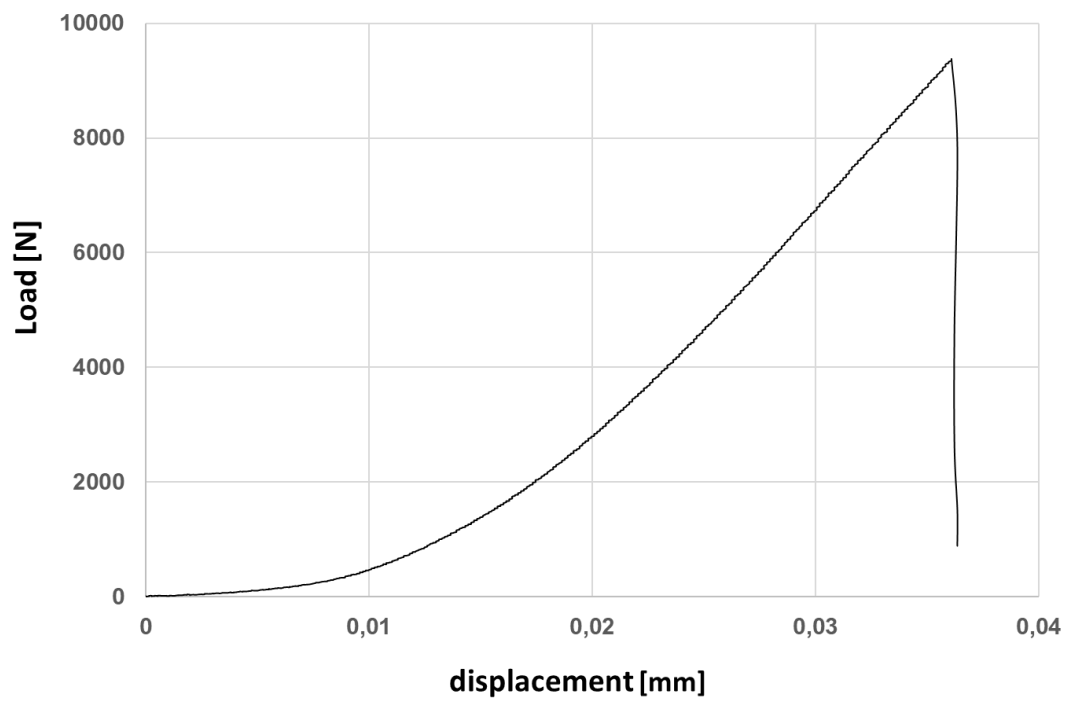


**Figure 9** Load/displacement curve of a CMC/ EN AW 6082 joint manufactured using SUP42 HT-2 by means of the standard joining process

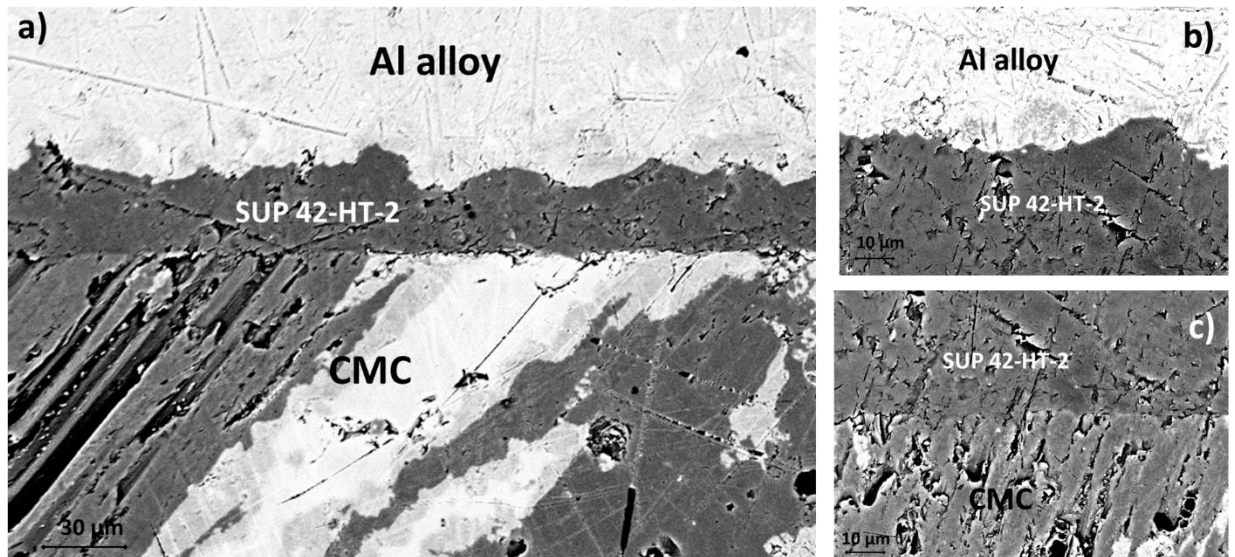


**Figure 10** SEM microscopy (a) of the cross –section of the CMC/ EN AW 6082 joint after the 240 h salt spray test; magnification of the adhesive/Al interface (b) and of the CMC/adhesive interface (c)

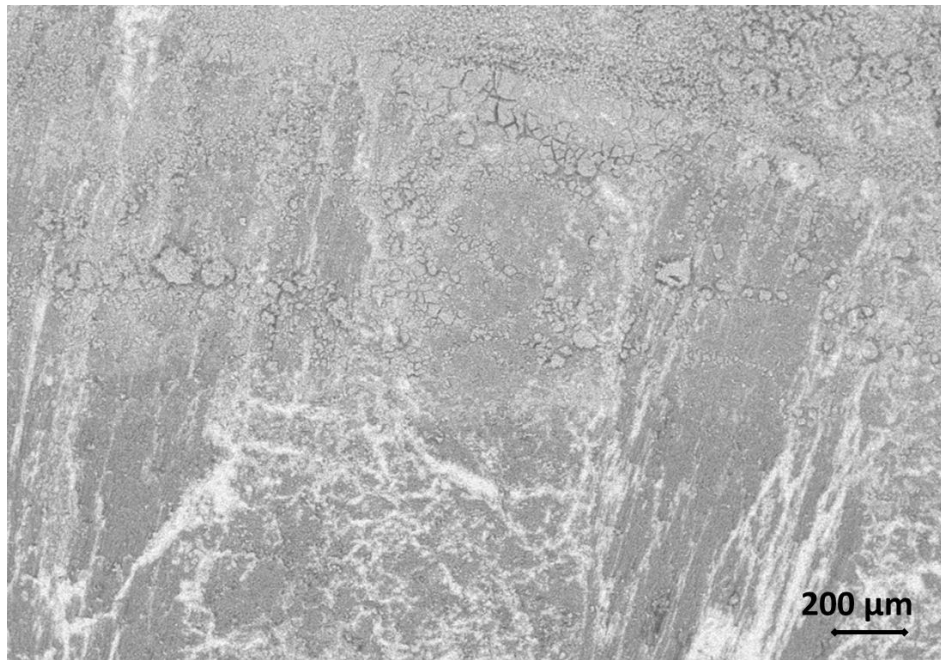


**Figure 11** Top view SEM magnification of an EN AW 6082 part after the 240 h salt spray test; the image refers to an Al alloy area outside the joint

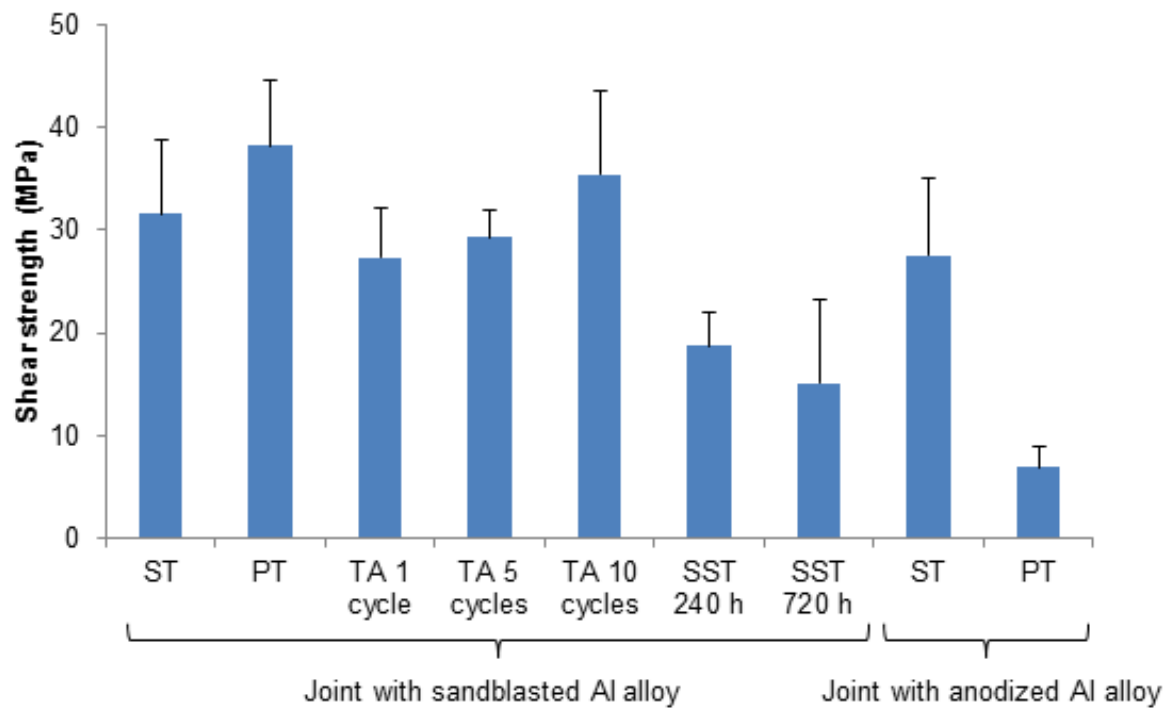


**Figure 12** Results of the mechanical tests. Legend: ST = standard treatment, PT = post-treatment at 200 °C/10 min, TA = thermal ageing at 200 °C (each cycle 1 min), SST = salt spraying tests.



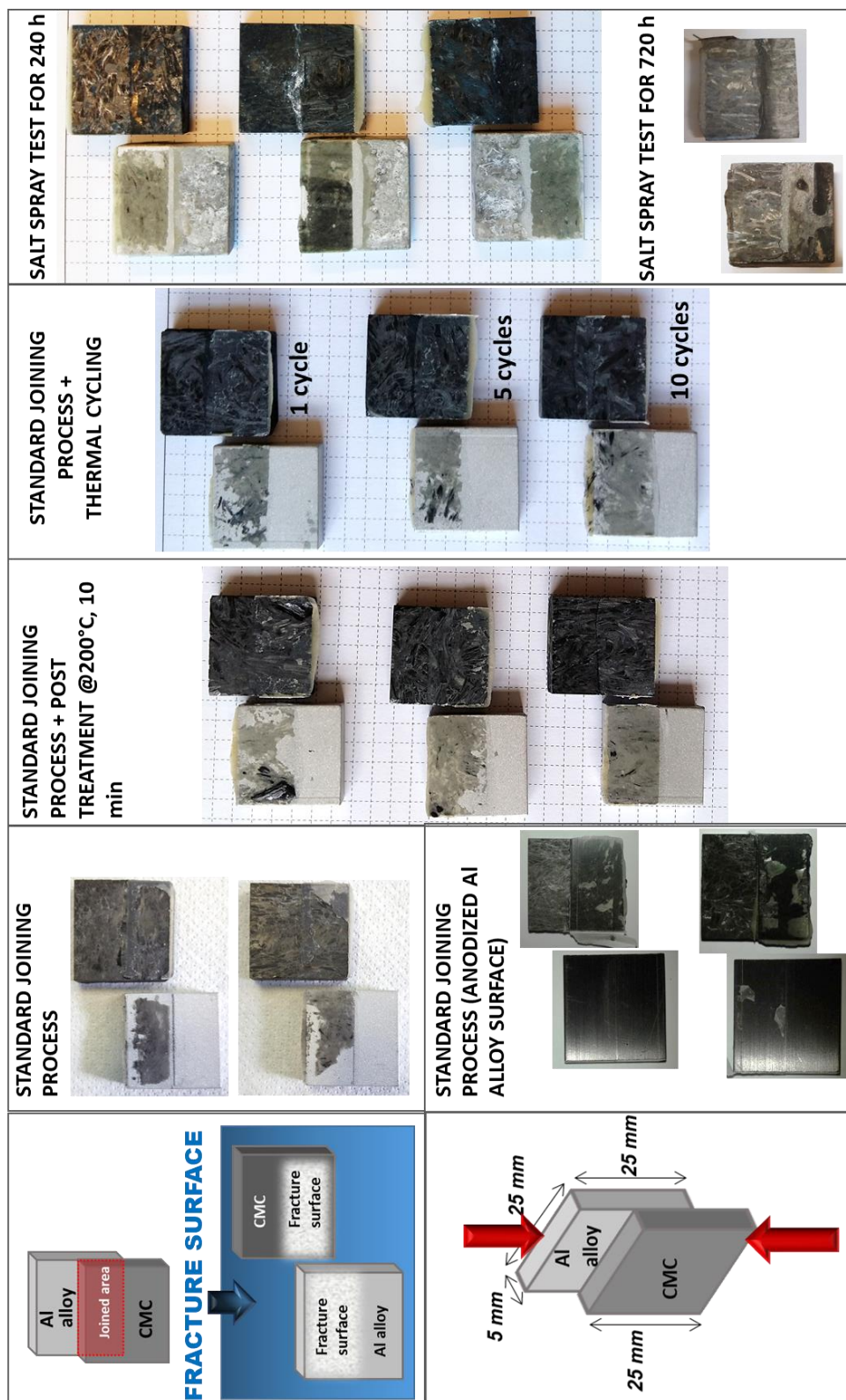


**Figure 13** Fracture surfaces of Al alloy/CMC samples joined with SUP 42 HT-2 after the SLO shear test (EN AW 6082 surface on the left and CMC surface on the right for each surface macrography )

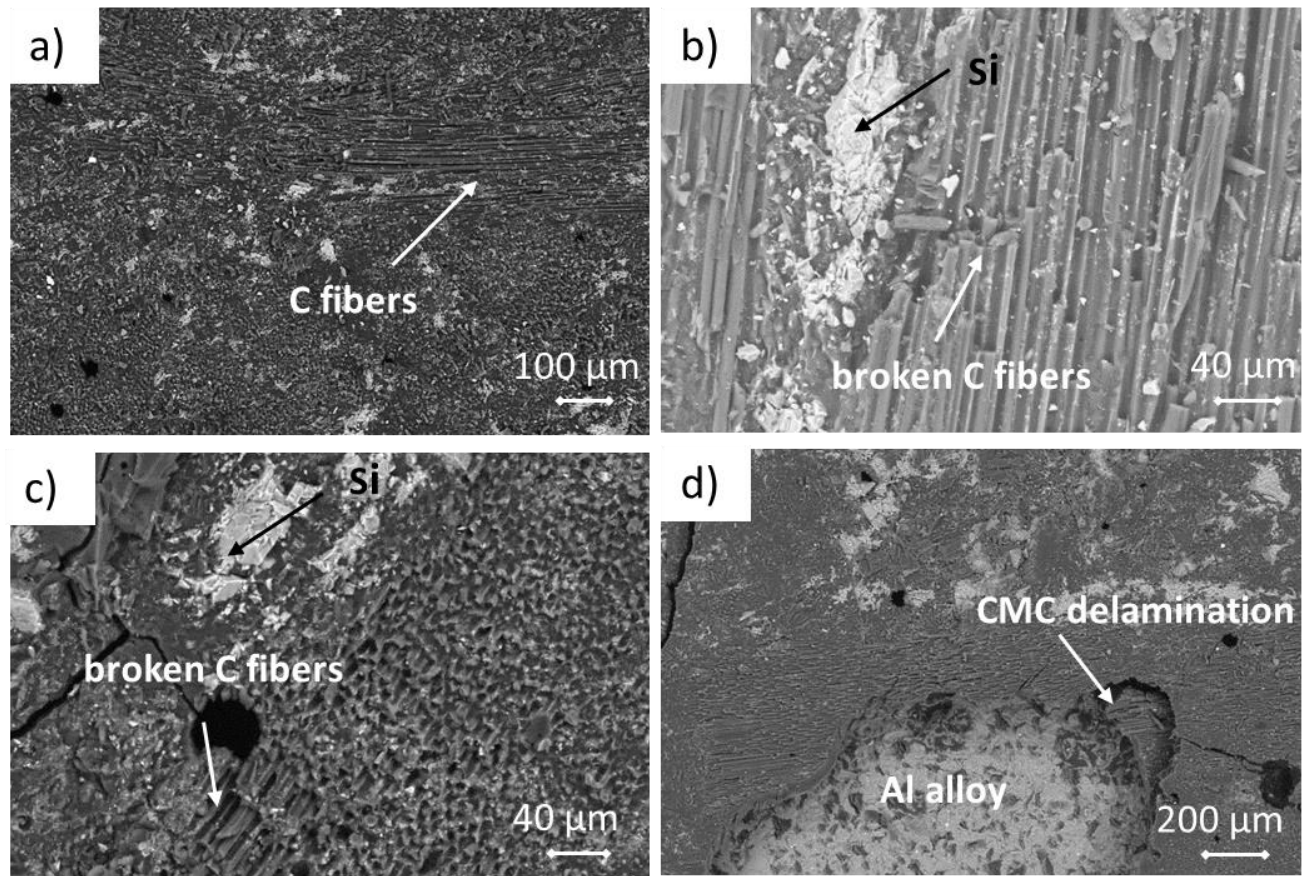


**Figure 14** SEM images of fracture surfaces of the CMC / EN AW 6082 joints (adhesive curing with post treatment at 200°C for 10 minutes) (Al alloy side) after the SLO shear test



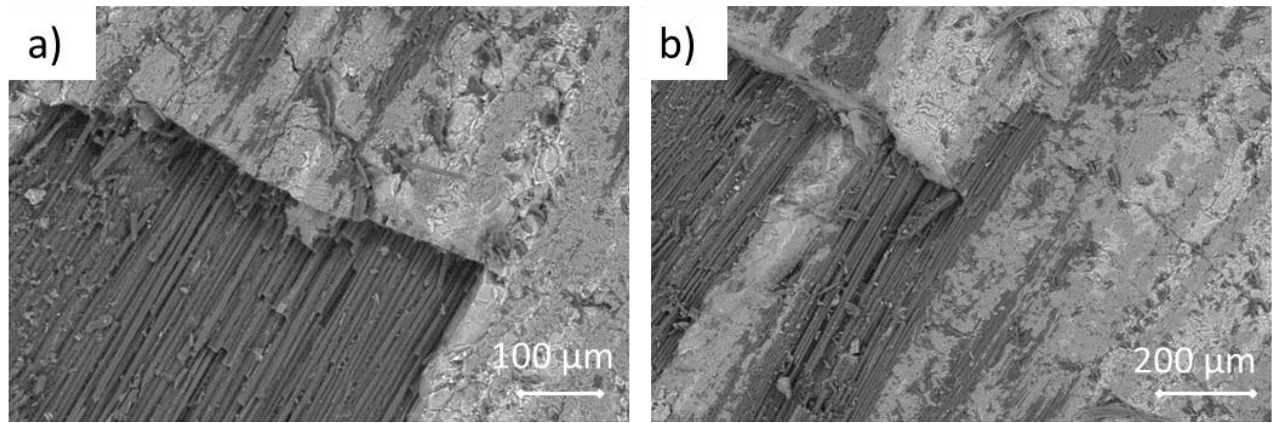


**Figure 15** SEM images of fracture surfaces of the CMC / EN AW 6082 joints  
(adhesive curing with post treatment at 200°C for 10 minutes) ( CMC side) after the  
SLO shear test; delamination of the composite is detectable

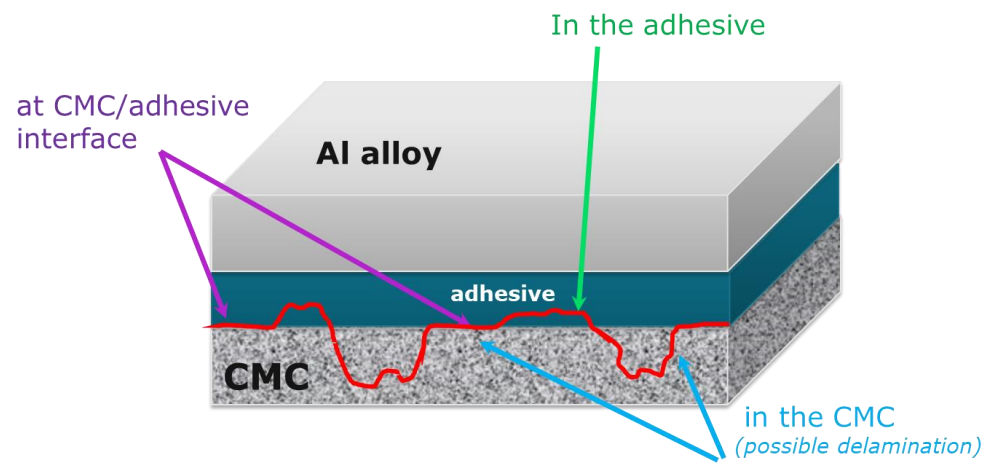


**Figure 16** A schematic of a possible fracture path in EN AW 6082 /CMC joints (but not for an anodized sample)

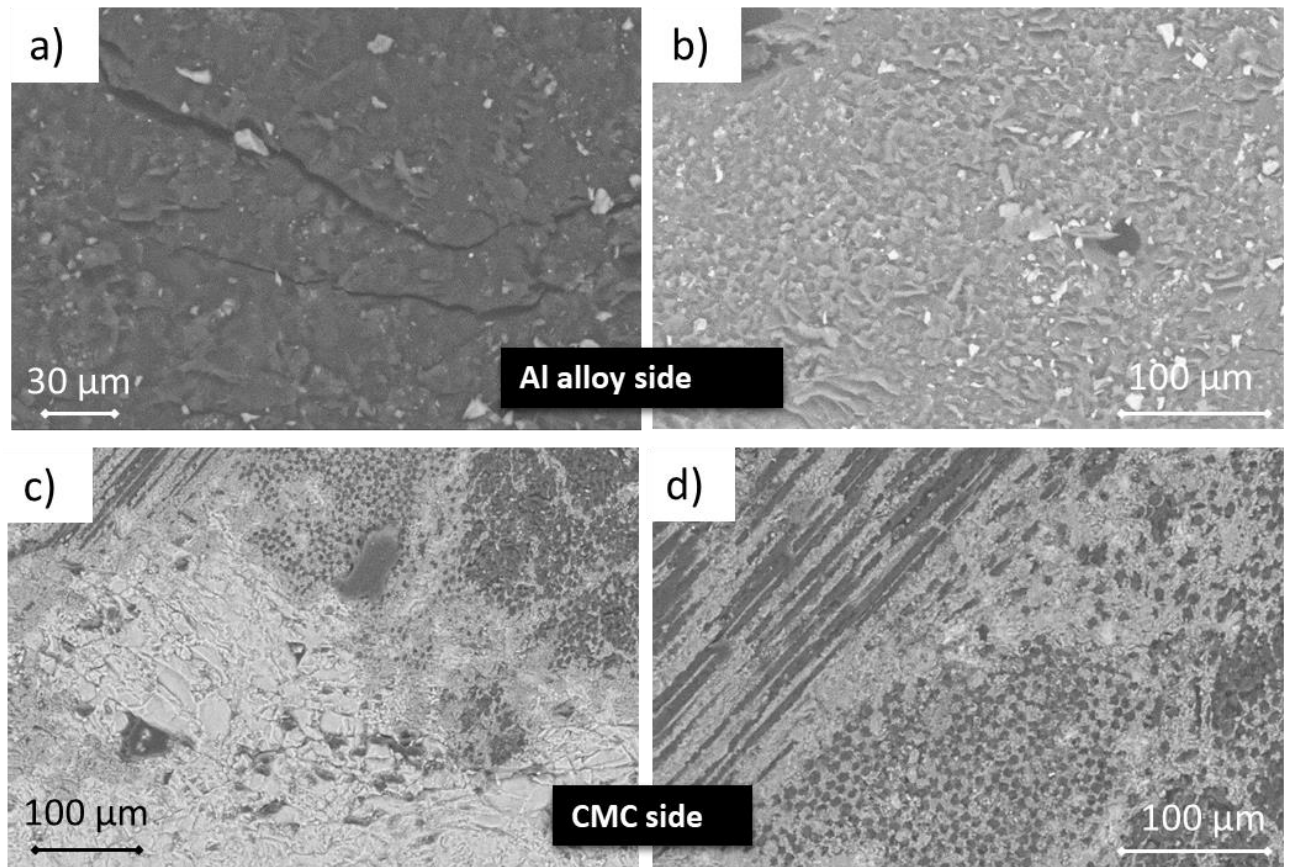


**Figure 17** SEM images of fracture surfaces of the tested joints after 10 cycles at 200°C and the SLO shear test

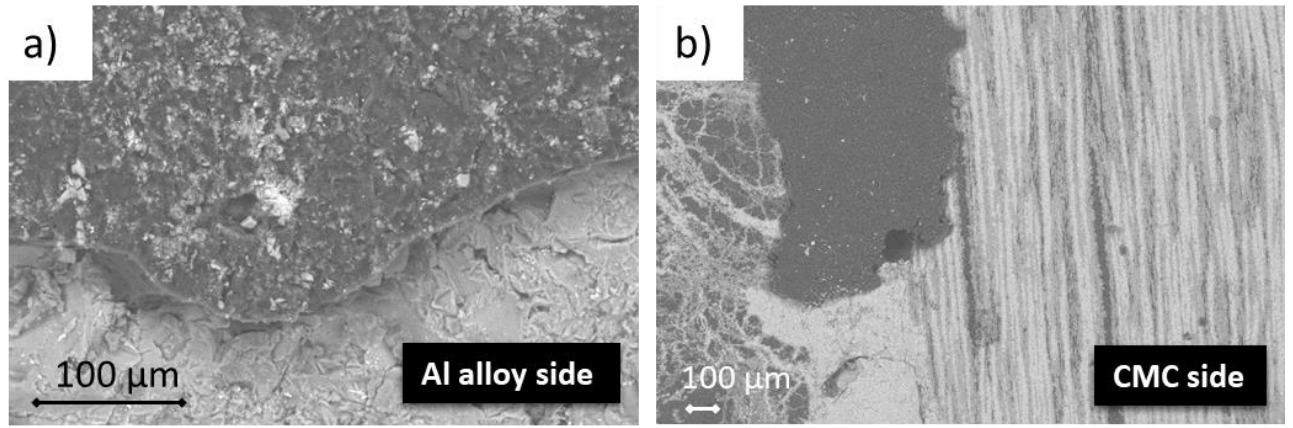


**Figure 18** SEM images of fracture surfaces of the tested joints after the 240 h salt spray test and SLO shear test

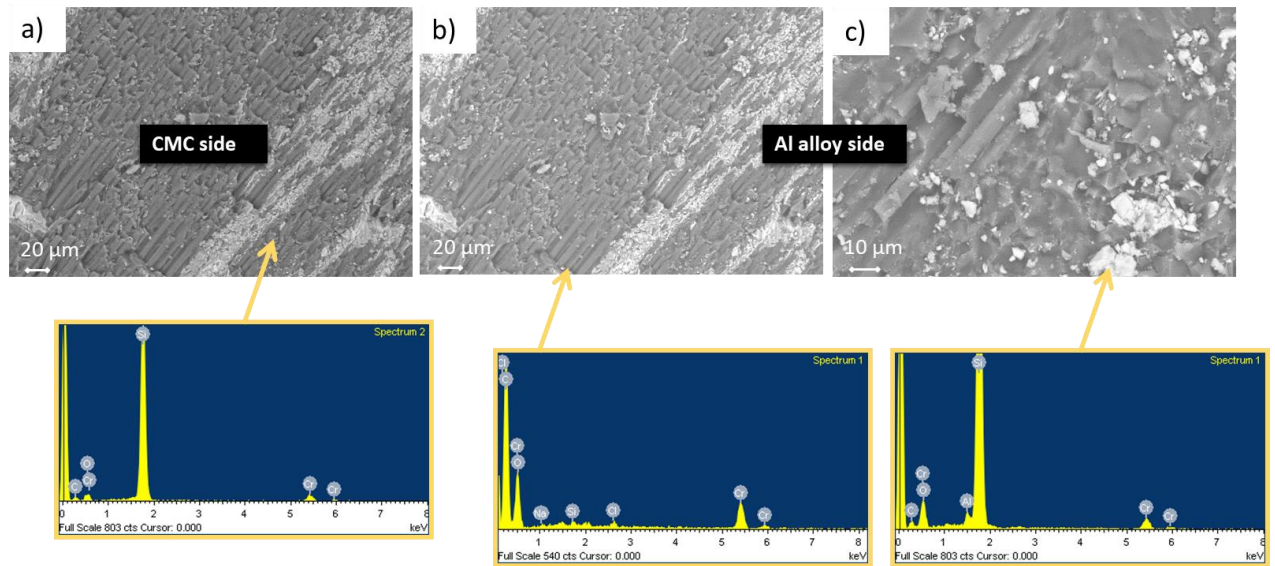


**Figure 19** SEM images of fracture surfaces of the tested joints after the 720 h salt spray test and SLO shear test ; compositional analysis of some areas is reported in the insets

